Selective counterion condensation in ionic micellar solutions

V. K. Aswal[1,*] and P. S. Goyal[2]

[1]*Spallation Neutron Source Division, Paul Scherrer Institut, CH-5232 PSI Villigen, Switzerland*
[2]*IUC-DAEF, Mumbai Centre, Bhabha Atomic Research Centre, Mumbai 400 085, India*

Small-angle neutron scattering experiments have been carried out on micellar solutions of cationic surfactants of cetyltrimethylammonium bromide (CTABr) and chloride (CTACl) in the presence of varying concentrations of salts KBr and KCl. In these systems, while the size of micelles strongly increases with the addition of KBr, the effect of addition of KCl in comparison is much less pronounced. It is found that in equimolar surfactant to salt micellar solutions of CTABr/KCl and CTACl/KBr, the micellar sizes are larger in CTACl/KBr than those in CTABr/KCl. The measurements have been done for different equimolar surfactant to salt concentrations and at different temperatures. We explain these results in terms of selective counterion condensation on the micelles. That is, while the condensation of Cl^- counterions on the CTABr micelles in CTABr/KCl takes place around the condensed Br^- counterions of CTABr, the Cl^- counterions of CTACl in CTACl/KBr are replaced by Br^- counterions of the salt. Similar results have also been obtained on micellar solutions of anionic surfactants of sodium dodecyl sulfate and lithium dodecyl sulfate in the presence of salts LiBr and NaBr, respectively.

I. INTRODUCTION

Surfactant molecules consist of two distinct segments that are opposite in character. One part is polar in character and is known as head group, while the other part is comprised of one or more long hydrophobic tails. These molecules in aqueous solution above a critical micelle concentration (CMC) are known to self-aggregate to form micelles [1,2]. Polar head groups of these aggregates lie near the bulk aqueous media, whereas the hydrocarbon tails extend inward to stay away from the unfavorable water contacts. The micelles are formed by the delicate balance of opposing forces: the attractive tail-tail hydrophobic interaction provides the driving force for the aggregation of surfactant molecules, while the electrostatic repulsion between the polar head groups limits the size that a micelle can attain. As a result, the characteristics of these aggregates are easily controlled by the changes in solution conditions such as temperature, concentration, and ionic strength [3–7]. The aggregates formed are of various types, shapes, and sizes such as spherical or ellipsoidal, cylindrical or threadlike, disklike micelle, membrane, and vesicle. The study of formation of these different structures is important as the surfactant solutions are widely used in various household, industrial, and research applications [8].

Surfactant molecules such as cetyltrimethylammonium bromide (CTABr) ionize in aqueous solution and the corresponding micelles are aggregates of CTA^+ ions. The micelle is charged and is called an ionic micelle. The Br^- ions, known as counterions, tend to stay near the CTA^+ micellar surface. The shape, size, fractional charge of the micelle, and the intermicellar interaction depend on the the nature of these counterions. It is well known that salts such as KBr and sodium salicylate induce pronounced growth of CTABr mi-

celles due to charge neutralization at the micellar surface by these salts [9,10]. The hydration of the counterions is important to decide the effect of salts on the growth of the micelles in these systems [11–13].

Since the works of Oosawa [14] and Manning [15], the concept of counterion condensation is widely accepted in the field of linear polyelectrolytes. It has been shown that when the charge density on an infinitely long cylinder is increased beyond a critical value, counterions condense around the cylinder so as to reduce the effective charge density to the critical value. Similar concepts have also been used in colloidal suspensions made of spherical charged colloids [16–18]. The counterions located at short enough distances from the colloidal surface feel a very strong electrostatic attraction compared with the thermal energy $k_B T$, and these counterions are called as bound to or condensed on the colloid. In ionic micellar solutions, the counterion condensation plays a very important role, as it decides the effective charge on the micelle and hence the formation, structure, and interaction of the micelle [19–22].

In this paper, we show the selective counterion condensation in ionic micellar solutions. It is known that the effect of addition of salts KBr and KCl to the ionic micellar solutions of cationic surfactant (e.g., CTABr or CTACl) is quite different [11,13,23]. In terms of counterion condensation, this suggests the differences in the condensation of Br^- and Cl^- ions that takes place on the charged micelles. We compare the structure in the equimolar surfactant to salt micellar solutions of CTABr/KCl and CTACl/KBr systems and explain the results in terms of selective counterion condensation. In particular, we show that CTACl/KBr micellar solution behaves like CTABr/KCl due to selectivity of counterion condensation. Similar results are also derived from the micellar solutions of anionic surfactants of sodium and lithium dodecyl sulfates. The technique of small-angle neutron scattering (SANS) has been used to study the structure and interaction in above micellar solutions.

─────────
*Permanent address: Solid State Physics Division, Bhabha Atomic Research Center, Mumbai 40085, India.
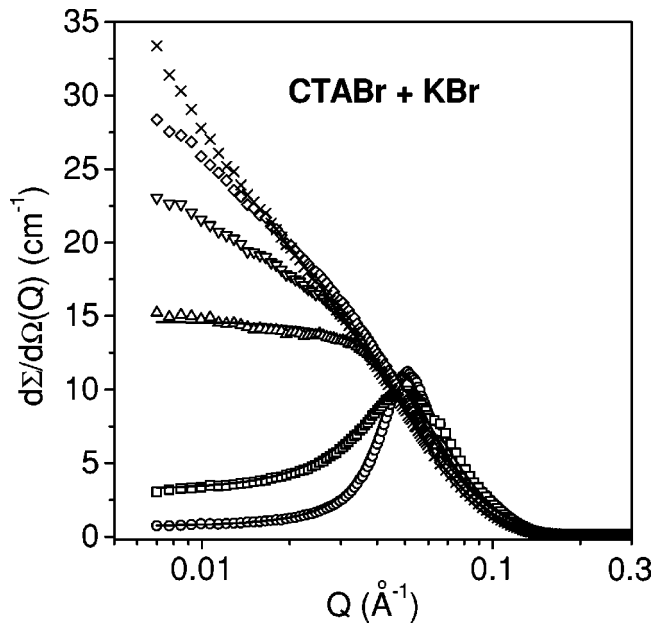
FIG. 1. SANS data from a micellar solution of 100 mM CTABr in the presence of varying KBr concentrations. The data from bottom to top correspond to the KBr concentrations of 0, 20, 40, 60, 80, and 100 mM, respectively.

II. EXPERIMENT

All the surfactants and salts were obtained from either Aldrich or Fluka and used as supplied. The samples for SANS experiments were prepared by dissolving known amount of surfactants and salts in D_2O. The use of D_2O as solvent instead of H_2O provides better contrast in neutron experiments. Small-angle neutron scattering experiments
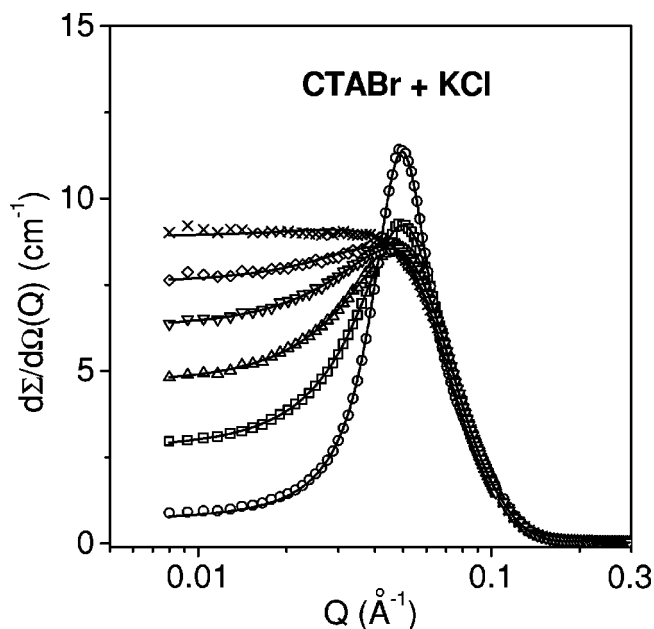

FIG. 3. SANS data from a micellar solution of 100 mM CTACl in the presence of varying KBr concentrations. The data from bottom to top correspond to the KBr concentrations of 0, 20, 40, 60, 80, and 100 mM, respectively.

were carried out using SANS diffractometer at the Swiss Spallation Neutron Source SINQ, Paul Scherrer Institut [24]. The wavelength of the neutron beam was 4.8 Å and the experiments were performed at two different samples to detector distances of 2 and 8 m to cover a Q range of 0.007 to 0.3 Å^{-1}. The scattered neutrons were detected using a two dimensional 96 cm$\times$96 cm detector. To find the structure

FIG. 2. SANS data from a micellar solution of 100 mM CTABr in the presence of varying KCl concentrations. The data from bottom to top correspond to the KCl concentrations of 0, 20, 40, 60, 80, and 100 mM, respectively.
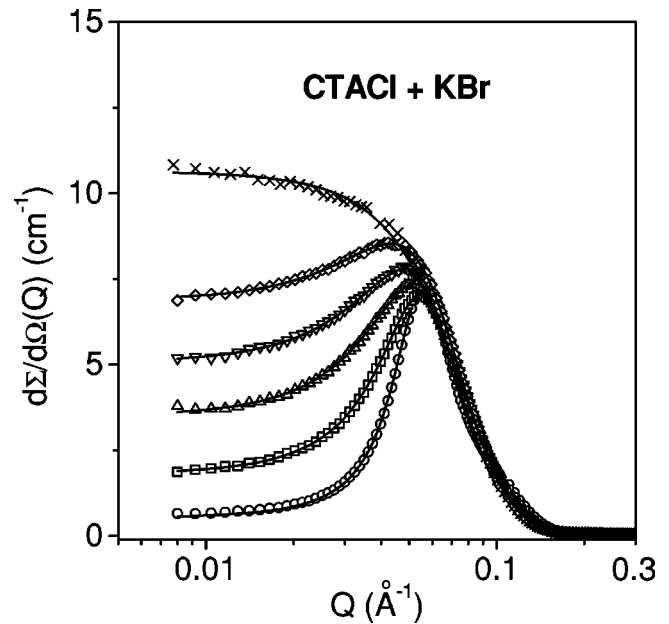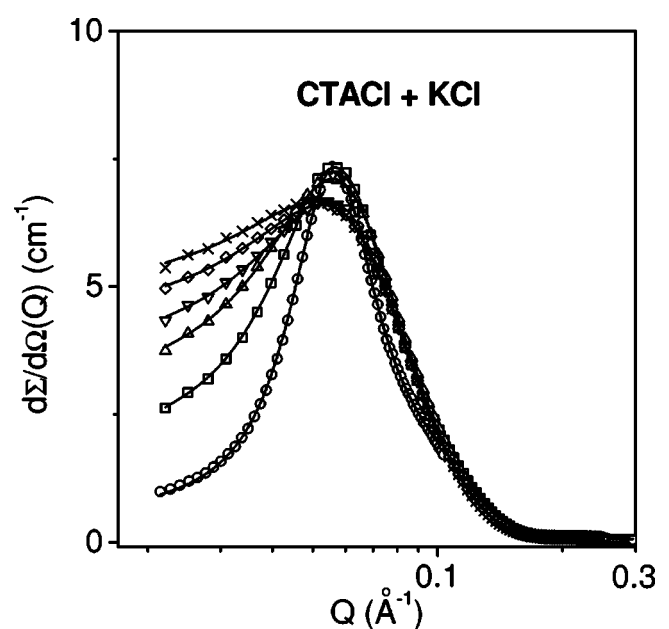

FIG. 4. SANS data from a micellar solution of 100 mM CTACl in the presence of varying KCl concentrations. The data from bottom to top correspond to the KCl concentrations of 0, 20, 40, 60, 80, and 100 mM, respectively.
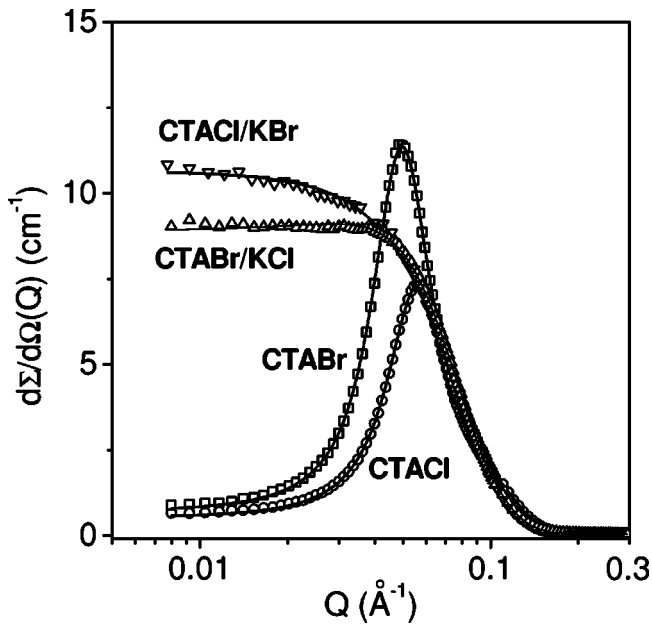
FIG. 5. SANS data from a 100 mM equimolar surfactant to salt micellar solutions of CTABr/KCl and CTACl/KBr. The data from 100 mM CTABr and CTACl micellar solutions without salt are also shown.

dependence of the micelles for different salts, SANS measurements were carried out on 100 mM micellar solutions of CTABr and CTACl in the presence of varying concentrations (0–100 mM) of KBr and KCl. The measurements on CTABr/KCl and CTACl/KBr micellar solutions to show the
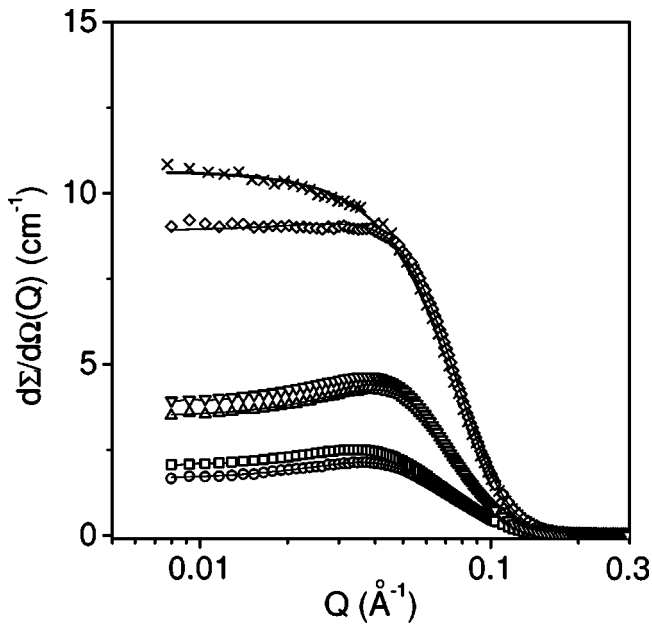

FIG. 6. SANS data from different equimolar surfactant to salt concentrations of CTABr/KCl and CTACl/KBr micellar solutions. The data pairs from bottom to top correspond to the concentrations of 25, 50, and 100 mM, respectively. For each concentration in the lower Q region the data of CTACl/KBr have higher cross section than CTABr/KCl.
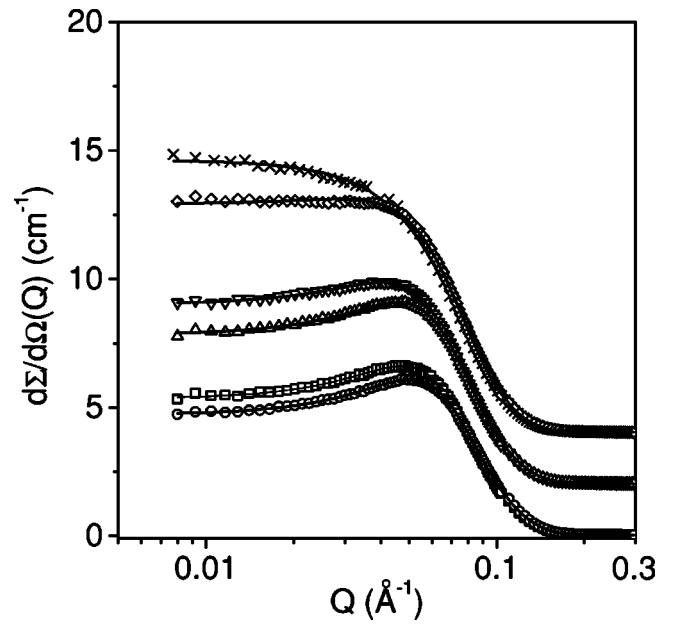

FIG. 7. SANS data from 100 mM equimolar surfactant to salt micellar solutions of CTABr/KCl and CTACl/KBr at different temperatures. The data pairs from top to bottom correspond to the temperatures of 30, 45, and 60 °C, respectively. The data of 30 and 45 °C are shifted vertically by four and two units, respectively.

selective counterion condensation were carried out for different equimolar surfactant to salt concentrations (25–100 mM) at fixed temperature (30 °C) and for one concentration (100 mM) at different temperatures (30–60 °C). Similar measurements were carried out on micellar solutions of anionic surfactants NaDS/LiBr and LiDS/NaBr for fixed equimolar surfactant to salt concentration (200 mM) and temperature (30 °C). The samples were held in a quartz sample holder of thickness 1 mm. The measured SANS data after standard corrections and normalizations are shown in Figs. 1–8.

III. SANS ANALYSIS

In SANS experiments, one measures the coherent differential scattering cross section per unit volume ($d\Sigma/d\Omega$) as a function of scattering vector Q. For a system of monodisperse interacting micelles $d\Sigma/d\Omega$ is given by [25]

$$\frac{d\Sigma}{d\Omega} = n(\rho_m - \rho_s)^2 V^2 \{\langle F^2(Q) \rangle + \langle F(Q) \rangle^2 [S(Q) - 1]\} + B,$$

(1)

where n denotes the number density of the micelles, ρ_m and ρ_s are, respectively, the scattering length densities of the micelle and the solvent, and V is the volume of the micelle. $F(Q)$ is the single particle form factor and $S(Q)$ is the interparticle structure factor. B is a constant term that represents the incoherent scattering background, which is mainly due to hydrogen in the sample.

The micelles formed at the critical micelle concentration are spherical. If the solution conditions (e.g., concentration, ionic strength, etc.) of the micellar solutions are changed to
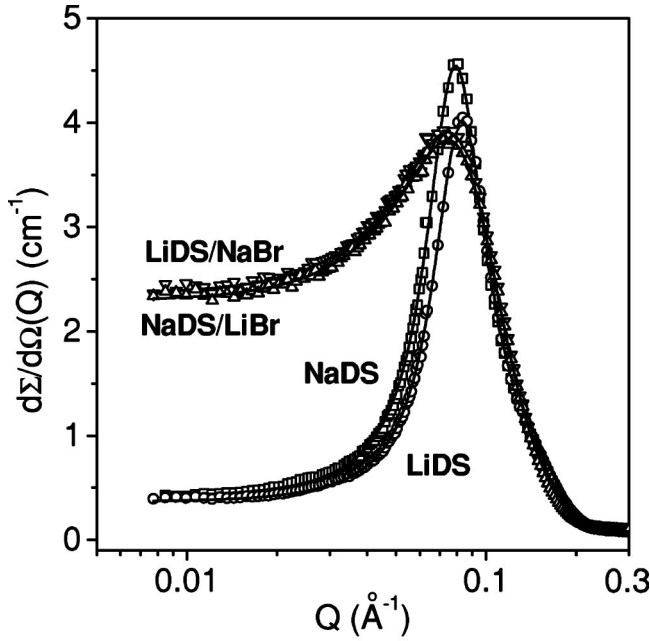
FIG. 8. SANS data from 200 mM equimolar surfactant to salt micellar solutions of NaDS/LiBr and LiDS/NaBr. The data from 200 mM NaDS and LiDS without salt are also shown.

favor the growth of the micelles, they grow along one of their axial directions. The growth of the micelles along other two axial directions is restricted by the length of the surfactant molecule to avoid any energetically unfavorable empty space or water penetration inside the micelle. The prolate ellipsoidal shape ($a \neq b = c$) of the micelles is widely used in the analysis of SANS data because it also represents the other different possible shapes of the micelles such as spherical ($a = b$) and rodlike ($a > b$). For such an ellipsoidal micelle

$$\langle F^2(Q) \rangle = \int_0^1 [F(Q,\mu)]^2 d\mu, \qquad (2)$$

$$\langle F(Q) \rangle^2 = \left[\int_0^1 [F(Q,\mu)] d\mu \right]^2, \qquad (3)$$

$$F(Q,\mu) = \frac{3(\sin x - x \cos x)}{x^3}, \qquad (4)$$

$$x = Q[a^2\mu^2 + b^2(1-\mu^2)]^{1/2}, \qquad (5)$$

where a and b are, respectively, the semimajor and semiminor axes of the ellipsoidal micelle and μ is the cosine of the angle between the directions of a and the wave vector transfer Q.

In general, micellar solutions of ionic surfactants show a correlation peak in the SANS data [26]. The peak arises because of the corresponding peak in the interparticle structure factor $S(Q)$ and indicates the presence of electrostatic interactions between the micelles. $S(Q)$ specifies the correlation between the centers of the different micelles and it is the

Fourier transform of the radial distribution function $g(r)$ for the mass centers of the micelle. Unlike the calculation of $F(Q)$, it is quite complicated to calculate $S(Q)$ for any other shape than spherical. This is because $S(Q)$ depends on the shape and orientation of the particles. To simplify this, prolate ellipsoidal micelles are assumed to be equivalent to spherical ones. We have calculated $S(Q)$ as derived by Hayter and Penfold from the Ornstein-Zernike equation and using the mean spherical approximation [27]. The micelle is assumed to be a rigid equivalent sphere of diameter $\sigma = 2(ab^2)^{1/3}$ interacting through a screened Coulomb potential, which is given by

$$u(r) = u_0 \sigma \frac{\exp[-\kappa(r-\sigma)]}{r}, \quad r > \sigma, \qquad (6)$$

where κ is the Debye-Hückel inverse screening length and is calculated by

$$\kappa = \left[\frac{8 \pi N_A e^2 I}{10^3 \epsilon k_B T} \right]^{1/2}, \qquad (7)$$

defined by the ionic strength I of the solution,

$$I = CMC + \frac{1}{2} \alpha (C - CMC) + C_s. \qquad (8)$$

I is determined by CMC, dissociated counterions from the micelles, and the salt concentration. The fractional charge α ($= Z/N$, where Z is the micellar charge and N is the aggregation number) is the charge per surfactant molecule in the micelle and is a measure of the dissociation of the counterions of the surfactant in the micelles. C and C_s present the concentrations of the surfactant and salt in the solution, respectively. The contact potential u_0 is given by

$$u_0 = \frac{Z^2 e^2}{\pi \epsilon \epsilon_0 \sigma (2 + \kappa \sigma)^2}, \qquad (9)$$

where ϵ is the dielectric constant of the solvent medium, ϵ_0 is the permittivity of free space, and e is the electronic charge.

Although micelles may produce polydisperse systems, we have assumed them as monodisperse for the simplicity of the calculation and to limit the number of unknown parameters in the analysis. The dimensions of the micelle, aggregation number, and the fractional charge have been determined from the analysis. The semimajor axis (a), semiminor axis ($b = c$), and the fractional charge (α) are the parameters in analyzing the SANS data. The aggregation number is calculated by the relation $N = 4\pi ab^2/3v$, where v is the volume of the surfactant monomer.

Throughout the data analysis, corrections were made for instrumental smearing [28]. For each instrumental setting the scattering profiles as given by Eq. (1) were smeared by the appropriate resolution function to compare with the measured data. The parameters in the analysis were optimized by means of nonlinear least-square fitting program and the errors on the parameters were calculated by the standard methods used [29].

TABLE I. Micellar parameters of 100 mM CTABr in the presence of varying concentrations of KBr and KCl.

Micellar system	Aggregation number N	Fractional charge α	Semiminor axis $b = c$ (Å)	Semimajor axis a (Å)	Axial ratio a/b
100 mM CTABr	174±9	0.23±0.01	24.0±0.5	40.2±1.2	1.68±0.04
100 mM CTABr + 20 mM KBr	210±10	0.17±0.01	24.6±0.5	44.6±1.2	1.81±0.04
100 mM CTABr + 40 mM KBr	366±20	0.05±0.01	24.6±0.5	81.0±3.0	3.29±0.04
100 mM CTABr + 20 mM KCl	189±9	0.19±0.01	24.6±0.5	41.8±1.2	1.70±0.04
100 mM CTABr + 40 mM KCl	197±10	0.17±0.01	24.6±0.5	43.6±1.2	1.77±0.04
100 mM CTABr + 60 mM KCl	202±10	0.16±0.01	24.6±0.5	44.7±1.2	1.82±0.04
100 mM CTABr + 80 mM KCl	206±11	0.14±0.01	24.6±0.5	45.6±1.2	1.85±0.04
100 mM CTABr + 100 mM KCl	208±11	0.11±0.01	24.6±0.5	46.0±1.2	1.87±0.04

IV. RESULTS AND DISCUSSION

Figure 1 shows the SANS data from 100 mM CTABr micellar solution in the presence of varying concentrations of KBr. The SANS distribution from a pure 100 mM CTABr shows a well defined correlation peak at the wave vector transfer $Q \sim 0.05$ Å^{-1}. This correlation peak is an indication of strong repulsive interaction between the positively charged CTABr micelles [26,30,31]. The peak usually occurs at $Q_m \sim 2\pi/d$, where d is the average distance between the micelles and Q_m is the value of Q at the peak position. In Fig. 1, the cross section increases and the peak position shifts to lower Q values with the increase in the salt concentration. This indicates the increase in the size of the micelles in the presence of salt. The broadening of the correlation peak is due to screening of charge by the salt between the micelles. The micellar parameters in these systems are given in Table I. It is seen that fractional charge on the micelle decreases and the aggregation number increases when the salt concentration in the micellar solution is increased. This suggests that the counterion condensation on the micelles increases as the salt is added. The charge neutralization at the surface of the micelle by the increase in the counterion condensation

decreases the effective head group area for the surfactant monomer to occupy in the micelle and hence the increase in the aggregation number of the micelle. The solid lines in Fig. 1 are the fitted curves to the experimental data using Eq. (1). It may be mentioned that the data are not fitted at higher salt concentrations (>40 mM) because of the complications in the calculation of $S(Q)$ for these data. SANS data do not show a correlation peak to fit a $S(Q)$ independent of $F(Q)$. The micelles in these systems are expected to carry a small charge, highly elongated and polydispersed [12].

Figure 2 shows the SANS data from 100 mM CTABr micellar solution in the presence of varying concentrations of KCl. The peak position and the cross section in these data do not change as much as for CTABr/KBr when the salt is added. For the same concentration of the salts KBr and KCl, the charge neutralization on the ionic CTABr micelles is different for these salts, and this leads to the formation of different micellar structures when KCl and KBr are added. For example, the aggregation number of CTABr micellar solution increases from 174 to 208 upon addition of 100 mM KCl; similar aggregation number upon addition of KBr is obtained only by the addition of 20 mM KBr (Table I).

TABLE II. Micellar parameters of 100 mM CTACl in the presence of varying concentrations of KBr and KCl.

Micellar system	Aggregation number N	Fractional charge α	Semiminor axis $b = c$ (Å)	Semimajor axis a (Å)	Axial ratio a/b
100 mM CTACl	115±6	0.28±0.01	23.0±0.5	29.1±1.0	1.27±0.04
100 mM CTACl + 20 mM KBr	140±5	0.24±0.01	23.4±0.5	34.2±1.0	1.46±0.04
100 mM CTACl + 40 mM KBr	165±6	0.21±0.01	24.0±0.5	38.3±1.0	1.60±0.03
100 mM CTACl + 60 mM KBr	187±9	0.19±0.01	24.6±0.5	41.3±1.2	1.68±0.03
100 mM CTACl + 80 mM KBr	208±11	0.17±0.01	24.6±0.5	46.0±1.4	1.87±0.04
100 mM CTACl + 100 mM KBr	228±12	0.06±0.02	24.6±0.5	50.4±1.6	2.05±0.04
100 mM CTACl + 20 mM KCl	127±7	0.26±0.01	23.2±0.5	31.6±1.0	1.36±0.04
100 mM CTACl + 40 mM KCl	135±7	0.26±0.01	23.2±0.5	33.5±1.0	1.44±0.04
100 mM CTACl + 60 mM KCl	140±7	0.26±0.01	23.2±0.5	34.8±1.0	1.50±0.04
100 mM CTACl + 80 mM KCl	144±7	0.25±0.01	23.4±0.5	35.2±1.0	1.51±0.04
100 mM CTACl + 100 mM KCl	147±8	0.25±0.01	23.4±0.5	35.9±1.0	1.53±0.04

TABLE III. Micellar parameters of CTABr, CTACl, and equimolar surfactant to salt solutions of CTABr/KCl and CTACl/KBr for different surfactant and salt concentrations.

Micellar system	Aggregation number N	Fractional charge α	Semiminor axis $b=c$ (Å)	Semimajor axis a (Å)	Axial ratio a/b
100 mM CTABr	174±9	0.23±0.01	24.0±0.5	40.2±1.2	1.68±0.04
100 mM CTACl	115±6	0.28±0.01	23.0±0.5	29.1±1.0	1.27±0.04
100 mM CTABr + 100 mM KCl	208±11	0.11±0.01	24.6±0.5	46.0±1.2	1.87±0.04
100 mM CTACl + 100 mM KBr	228±12	0.06±0.02	24.6±0.5	50.4±1.6	2.05±0.04
50 mM CTABr	150±8	0.26±0.01	24.0±0.5	34.8±1.0	1.45±0.04
50 mM CTACl	110±6	0.28±0.01	23.0±0.5	27.8±1.0	1.21±0.04
50 mM CTABr + 50 mM KCl	177±9	0.20±0.01	24.6±0.5	39.1±1.2	1.59±0.04
50 mM CTACl + 50 mM KBr	198±10	0.18±0.01	24.6±0.5	43.8±1.2	1.78±0.04
25 mM CTABr	137±7	0.26±0.01	24.0±0.5	31.8±1.0	1.33±0.04
25 mM CTACl	105±6	0.29±0.01	23.0±0.5	26.5±1.0	1.15±0.04
25 mM CTABr + 25 mM KCl	160±9	0.20±0.02	24.6±0.5	35.4±1.2	1.44±0.04
25 mM CTACl + 25 mM KBr	180±9	0.18±0.02	24.6±0.5	39.8±1.2	1.62±0.04

Figures 3 and 4 show the SANS data from a 100 mM CTACl micellar solution in the presence of varying concentrations of KBr and KCl, respectively. The SANS distribution from a pure 100 mM CTACl shows a well defined correlation peak similar to that in CTABr, but at the higher value of Q (~0.06 Å^{-1}). This suggests that in CTACl smaller micelles are formed as compared to those in CTABr. The differences in the micellar structure of the CTABr and CTACl are expected to be due to the differences in the counterion condensation of Br$^-$ and Cl$^-$ ions that takes place on the charged CTA$^+$ micelles. This is supported by the fact that fractional charge on micelles of CTABr is less than those on CTACl micelles. The effect of addition of salts KBr and KCl on CTACl micellar solution (Table II) shows similar trends to that on CTABr micellar solution (Table I). That is, while sizes of both CTABr and CTACl micelles increase strongly with the addition of KBr, the effect of KCl is much less pronounced.

The SANS data from equimolar surfactant to salt CTABr/KCl and CTACl/KBr micellar solutions as selected from Figs. 2 and 3 are shown in Fig. 5. These systems have common in them the same number of surfactant CTA$^+$ ions and as well as Br$^-$ and Cl$^-$ counterions. The comparison of micellar parameters on equimolar surfactant to salt solutions of CTABr/KCl (Table I) and CTACl/KBr (Table II) shows that the counterion condensation is more effective in CTACl/KBr than CTABr/KCl. We believe that this is due to selective condensation of the counterions around the micelles. In CTABr/KCl, Br$^-$ counterions from the dissociated CTABr molecules are condensed on the CTA$^+$ charged micelles. The condensation of Cl$^-$ ions of the salt KCl takes place around the condensed Br$^-$ ions. However, in CTACl/KBr, Cl$^-$ counterions of the CTACl molecules are replaced by Br$^-$ ions of KBr in the micelle. This is expected since Cl$^-$ ions are less effective than Br$^-$ in neutralizing the charge on the micelles [7,14]. The condensation of Br$^-$ ions around the condensed

TABLE IV. Micellar parameters of 100 mM CTABr, 100 mM CTACl, and corresponding equimolar surfactant to salt solutions of CTABr/KCl and CTACl/KBr at different temperatures.

Temperature T (°C)	Micellar system	Aggregation number N	Fractional charge α	Semiminor axis $b=c$ (Å)	Semimajor axis a (Å)	Axial ratio a/b
30	CTABr	174±9	0.23±0.01	24.0±0.5	40.2±1.2	1.68±0.04
30	CTACl	115±6	0.28±0.01	23.0±0.5	29.1±1.0	1.27±0.04
30	CTABr/KCl	208±11	0.11±0.01	24.6±0.5	46.0±1.2	1.87±0.04
30	CTACl/KBr	228±12	0.06±0.02	24.6±0.5	50.4±1.6	2.05±0.04
45	CTABr	143±7	0.26±0.01	23.0±0.5	36.2±1.0	1.57±0.04
45	CTACl	107±6	0.31±0.01	22.0±0.5	29.6±1.0	1.35±0.04
45	CTABr/KCl	167±9	0.20±0.01	23.6±0.5	40.1±1.0	1.70±0.04
45	CTACl/KBr	189±10	0.16±0.01	23.6±0.5	45.4±1.0	1.92±0.04
60	CTABr	122±7	0.28±0.01	22.0±0.5	33.7±1.0	1.53±0.04
60	CTACl	97±5	0.32±0.02	21.0±0.5	29.4±1.0	1.40±0.04
60	CTABr/KCl	141±8	0.23±0.01	22.6±0.5	36.9±1.2	1.63±0.04
60	CTACl/KBr	157±8	0.20±0.01	22.6±0.5	41.1±1.2	1.82±0.04

TABLE V. Micellar parameters of 200 mM NaDS, 200 mM LiDS, and corresponding equimolar surfactant to salt solutions of NaDS/LiBr and LiDS/NaBr.

Micellar system	Aggregation number N	Fractional charge α	Semiminor axis $b=c$ (Å)	Semimajor axis a (Å)	Axial ratio a/b
200 mM NaDS	83 ± 6	0.36 ± 0.02	16.7 ± 0.5	24.9 ± 1.0	1.49 ± 0.05
200 mM LiDS	72 ± 4	0.42 ± 0.02	16.7 ± 0.5	21.6 ± 0.8	1.29 ± 0.05
200 mM NaDS + 200 mM LiBr	100 ± 6	0.26 ± 0.02	16.7 ± 0.5	30.0 ± 1.2	1.80 ± 0.05
200 mM LiDS + 200 mM NaBr	101 ± 6	0.26 ± 0.02	16.7 ± 0.5	30.3 ± 1.2	1.81 ± 0.05

Cl^- counterions does not seem possible in CTACl/KBr as this, contrary to the experimental results, would make the counterion condensation less effective in CTACl/KBr than CTABr/KCl to neutralize the charge on the micelles. Similar results have also been obtained on the different equimolar surfactant to salt concentrations and at different temperatures. Figure 6 shows the SANS data on the different equimolar surfactant to salt concentrations of 25, 50, and 100 mM of CTABr/KCl and CTACl/KBr at a constant temperature of 30 °C. The temperature dependence for 100 mM equimolar surfactant to salt concentration of CTABr/KCl and CTACl/KBr at different temperatures 30, 45, and 60 °C is shown in Fig. 7. The calculated micellar parameters in these systems for different concentrations and temperatures are given in Tables III and IV, respectively. The higher values of the charge neutralization on the micelles and the micellar sizes in CTACl/KBr than those in CTABr/KCl can be explained in terms of a small fraction of condensed Cl^- counterions that are not replaced by Br^- in the micelles of CTACl/KBr solutions [14]. This provides less fractional charge on the micelles of CTACl/KBr than CTABr/KCl, otherwise these two systems have similar counterion condensation of Br^- and Cl^- ions around them.

Figure 8 shows the SANS data on equimolar surfactant to salt micellar solutions of anionic surfactants NaDS and LiDS (DS, dodecyl sulfate) in the presence of LiBr and NaBr, respectively. For comparison, the micellar solutions from pure NaDS and LiDS are also shown in Fig. 8. It is found that while the SANS data on pure NaDS and LiDS are significantly different, the equimolar surfactant to salt solutions of NaDS/LiBr and LiDS/NaBr are similar. The micellar parameters in these systems are given in Table V. These results are similar to those on cationic surfactants and support the selective counterion condensation in ionic micellar solutions. We believe that in LiDS/NaBr micellar solution, Li^+ counterions are replaced by Na^+ counterions, so that this systems has the

similar counterion condensation to that of NaDS/LiBr. The Na^+ ions are preferred on the micellar surface due to their less hydrophilicity as compared to Li^+ ions [7,14].

The hydrated size of the counterion plays an important role in deciding the effect of salt on the structure and interaction in the micellar solutions. From a theoretical point of view, the most commonly used model to understand the counterion condensation around the charged particles is the Poisson-Boltzmann (PB) model [16–18]. However, this model does not take into account the finite size of the condensed counterions. As a result, this model does not distinguish the effect of counterions with different sizes when they have the same valency. Several attempts have been proposed to include the steric repulsion in order to improve the PB model [32]. One of the most recent work [33], which takes account of the finite size of the ions, suggests that the concentration of condensed counterions tends to saturate to the value $1/r_c^3$ and the layer thickness of the condensed counterions is proportional to r_c^3, where r_c is the hydrated size of the counterion. This means that the counterion condensation will increase when the hydrated size is small and vice versa. Counterions Br^- and Na^+ ions are less hydrated than Cl^- and Li^+, respectively, and hence they are more effective and preferred on the selective counterion condensation.

V. CONCLUSIONS

SANS studies have been carried out on ionic micellar solutions of CTABr, CTACl, NaDS, and LiDS in the presence of different salts. The comparison of micelle structures in equimolar surfactant to salt micellar solutions of CTACl/KBr and CTABr/KCl or NaDS/LiBr and LiDS/NaDS suggests the selective counterion condensation in these systems. The counterions with large hydrated size are replaced by the ones with less hydrated size.

[1] C. Tanford, *The Hydrophobic Effect: Formation of Micelles and Biological Membranes* (Wiley, New York, 1980).

[2] H. Wennerstrom and B. Lindman, Top. Curr. Chem. **87**, 1 (1980).

[3] V. Degiorgio and M. Corti, *Physics of Amphiphiles: Micelles, Vesicles and Microemulsion* (North-Holland, Amsterdam, 1985).

[4] S.H. Chen, Annu. Rev. Phys. Chem. **37**, 351 (1986).

[5] R. Zana, *Surfactant Solutions: New Methods of Investigations* (Dekker, New York, 1987).

[6] Y. Chevalier and T. Zemb, Rep. Prog. Phys. **53**, 279 (1990).

[7] J.N. Israelachvili, *Intermolecular and Surface Forces* (Academic Press, New York, 1992).

[8] J.M. Schnur, Science (Washington, DC, U.S.) **262**, 1669

(1993).

[9] M. Cates and S.J. Candau, J. Phys.: Condens. Matter **2**, 6869 (1990).

[10] H. Rehage and H. Hoffman, Mol. Phys. **74**, 933 (1991).

[11] V.K. Aswal, P.S. Goyal, S.V.G. Menon, and B.A. Dasannacharya, Physica B **213**, 607 (1995).

[12] V.K. Aswal, P.S. Goyal, and P. Thiyagarajan, J. Phys. Chem. B **102**, 2469 (1998).

[13] V.K. Aswal and P.S. Goyal, Phys. Rev. E **61**, 2947 (2000).

[14] F. Oosawa, *Polyelectrolytes* (Dekker, New York, 1971).

[15] G.S. Manning, J. Chem. Phys. **51**, 924 (1969).

[16] S. Alexander, P.M. Chaikin, P. Grant, G.J. Morales, P. Pincus, and D. Hone, J. Chem. Phys. **80**, 5776 (1984).

[17] G.V. Ramanathan, J. Chem. Phys. **88**, 3887 (1988).

[18] L. Belloni, Colloids Surf., A **140**, 227 (1998).

[19] V.K. Aswal, P.S. Goyal, S. De, S. Bhattacharya, H. Amenitsch, and S. Bernstorff, Chem. Phys. Lett. **329**, 336 (2000).

[20] V.K. Aswal and P.S. Goyal, Chem. Phys. Lett. **357**, 491 (2002).

[21] V.K. Aswal and P.S. Goyal, Chem. Phys. Lett. **364**, 44 (2002).

[22] J.V. Joshi, V.K. Aswal, P. Bahadur, and P.S. Goyal, Curr. Sci. India **83**, 47 (2002).

[23] P.S. Goyal, S.V.G. Menon, B.A. Dasannacharya, and V. Raja-

gopalan, Chem. Phys. Lett. **211**, 559 (1993).

[24] J. Kohlbrecher and W. Wagner, J. Appl. Crystallogr. **33**, 804 (2000).

[25] S.H. Chen and T.L. Lin, in *Methods of Experimental Physics*, edited by D.L. Price and K. Skold (Academic Press, New York, 1987), Vol. 23B, p. 489.

[26] S.H. Chen, E.Y. Sheu, J. Kalus, and H. Hoffmann, J. Appl. Crystallogr. **21**, 751 (1988).

[27] J.B. Hayter and J. Penfold, Colloid Polym. Sci. **261**, 1022 (1983).

[28] J.S. Pedersen, D. Posselt, and K. Mortensen, J. Appl. Crystallogr. **23**, 321 (1990).

[29] P.R. Bevington, *Data Reduction and Error Analysis for Physical Sciences* (McGraw-Hill, New York, 1969).

[30] V.K. Aswal and P.S. Goyal, Physica B **245**, 73 (1998).

[31] V.K. Aswal, S. De, P.S. Goyal, S. Bhattacharya, and R.K. Heenan, Phys. Rev. E **57**, 776 (1998).

[32] A.G. Volkov, D.W. Deamer, D.L. Tanelian, and V.S. Mirkin, Prog. Surf. Sci. **53**, 1 (1997), and references therein.

[33] I. Borukhov, D. Andelman, and H. Orland, Phys. Rev. Lett. **79**, 435 (1997).